Cracking of epitaxial MnAs films on GaAs(001)

Y. Takagaki,[1,a)] M. Moreno,[2] P. Schützendübe,[1] M. Ramsteiner,[1] and C. Herrmann[1]
[1]*Paul-Drude-Institut für Festkörperelektronik, Hausvogteiplatz 5-7, 10117 Berlin, Germany*
[2]*Instituto de Ciencia de Materiales de Madrid (CSIC), Cantoblanco, 28049 Madrid, Spain*

(Received 24 July 2009; accepted 10 December 2009; published online 25 January 2010)

We report the characteristics of the fracture of epitaxially grown MnAs films on GaAs(001) due to the large thickness or induced by annealing. Stresses arising from the thermal expansion mismatch and the structural phase transition can no longer be accommodated when the film thickness is beyond about 0.5 μm, giving rise to cracking of the films. The cracks are inclined with respect to the *c* axis of MnAs, suggesting their initiation by a weak plane. For films thicker than about 2 μm, the fracture extends to the substrates, where the in-plane crack angle changes from about 57° to around 45° as the cracking is dictated by the cleavage plane of the substrates. Even for films much thinner than 0.5 μm, annealing results in a delamination from substrate as a consequence of the large thermal expansion and, plausibly, the oxidation of MnAs. We show that Mn capping suppresses the delamination as well as the oxidation during the annealing. © *2010 American Institute of Physics*. [doi:10.1063/1.3288993]

I. INTRODUCTION

In heteroepitaxial growth, the relief of stress in overgrown films imposed by the substrates is a crucial issue when the film thickness is required to be large. Stresses can be relieved through several mechanisms in thin films. However, the excessive stress in thick films forces cracking of the films and even of the substrates. Understanding the mechanism of the cracking and subsequently preventing its occurrence are of great importance in a wide variety of applications. Continuum models have been developed to explain general behaviors of the fractures.[1,2] The fractures are governed by the strain energy release rate,

$$G = Z\sigma_f^2 h/E_f, \tag{1}$$

where σ_f is the stress in the film, h is the film thickness, E_f is the modulus of elasticity, and Z is a dimensionless cracking parameter. A fracture occurs in the film, interface, or substrate when G exceeds the toughness of the respective part.

Here, we investigate the cracking behavior of MnAs films epitaxially grown on the GaAs substrates. MnAs is a ferromagnetic material having a hexagonal crystal structure.[3] The material is prospective for spintronic applications as Curie temperature T_C(≈40 °C) is above room temperature and epitaxial growth on GaAs and Si is possible.[4] The fracture of films is particularly significant for MnAs due to its large thermal expansion. The films crack during the cooling following growth when the thickness exceeds about 0.5 μm.[5] Even if the thickness is smaller than 0.5 μm, cracking and/or delamination[6] are encountered when the films are annealed. We emphasize that, due to the low growth temperature (typically 220–270 °C), even an annealing at moderate temperatures can cause delamination in originally uncracked films.

We show that the cracking in the MnAs/GaAs system is almost confined in the films when the thickness is below 2 μm. For films thicker than 2 μm, the fracture massively extends to the substrates, leading to detachment of MnAs/GaAs composite flakes. We pay particular attention to deviations in the fracture behavior from the expectations of the continuum models, which arise owing to the single crystallinity of the system. Additionally, we demonstrate that Mn capping allows us to circumvent the delamination of the films during annealing.

II. EXPERIMENTS

Solid-source molecular-beam epitaxy was employed to grow MnAs films having thicknesses of up to 3 μm at growth temperatures of about 250 °C.[4,5] The GaAs substrates were (001) oriented, and so the epitaxial orientation of the MnAs films was principally $(1\bar{1}00)$. The [0001] and $[11\bar{2}0]$ directions of the MnAs films were aligned along the $[1\bar{1}0]$ and [110] directions of the GaAs substrates, respectively. Annealing of MnAs films was carried out in a nitrogen atmosphere at a temperature of 400 °C for 10 min, unless stated otherwise. MnAs oxidizes at relatively low temperatures. To demonstrate suppression of the oxidation as well as delamination, a 25-nm-thick MnAs film was capped by a Mn layer at a temperature of −26 °C. The nominal thickness of the Mn layer was 10 nm.

III. CRACKING OF THICK FILMS

A. Film fracture regime

The critical thickness h_c for cracking is about 0.5 μm for MnAs films on GaAs(001).[5] When the thickness is just beyond h_c, the MnAs films are observed to split perpendicular to the *c* axis of MnAs, as shown in Fig. 1(a). (In the following, we refer to this form of cracking as type I.) The fracture occurs in the manner of a quasiperiodic array of parallel cracks. The period is typically about 10 μm. Theoretically,[1,2,7] the critical thickness for the splitting of a film is given by $h_c = 0.5K_f^2/\sigma_c^2$, where σ_c is the critical stress

a)Electronic mail: takagaki@pdi-berlin.de.

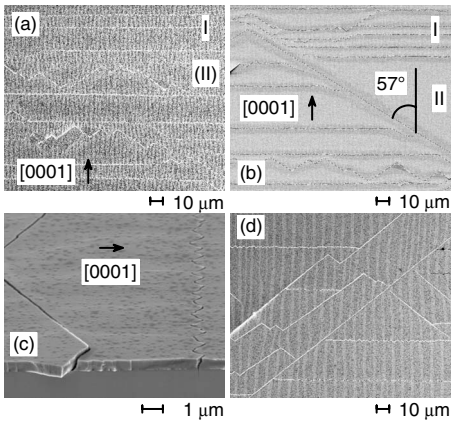

FIG. 1. Scanning electron micrographs of MnAs films on GaAs(001). The two types of cracks I and II are labeled. The film thickness is 0.69 μm in (a) and (b), 0.66 μm in (c), and 1.8 μm in (d). The *c*-axis of MnAs is aligned in the vertical direction in (a), (b), and (d) and in the horizontal direction in (c). The type-I cracks which are nominally orthogonal to the *c*-axis of MnAs consist of short inclined segments as shown by the right-hand-side crack in (c). The vertical stripe in (a) is due to the alternating narrow segments of α- and β-MnAs. In (b), the elastic deformation associated with the strain relaxation resulted in a darkening in the contrast in narrow strips adjacent to the cracks.

and K_f is the fracture toughness of the film. The crack spacing is predicted to be about eight times the film thickness, which is about a half of the experimental result. The slight discrepancy is reasonable as the cracks are immobile and thus cannot be ideally incorporated in real situation for optimal relief of the stress. As a matter of fact, the strain relaxation in the vicinity of the cracks can be visible in scanning electron microscopy under an appropriate configuration of the detector. In Fig. 1(b), one finds that the surface deformation associated with the cracking has yielded a darkening in the contrast. The width of the strain-relaxed area is directly confirmed to be as expected by the theory.

The cracking perpendicular to the *c*-axis can be understood as follows. For epitaxial MnAs films on GaAs substrates, the stress originating from the mismatch in the lattice constants is almost completely compensated during the growth by the introduction of misfit dislocations. The thermal expansion coefficient of MnAs is about one order of magnitude larger than that of GaAs. The films are hence tensile stressed when the temperature is lowered to room temperature after the growth. In the case of MnAs films, the critical thickness is modified because of the first-order structural phase transition that accompanies the magnetic phase transition at $T_C(\approx 40\ ^\circ\mathrm{C})$. At the phase transition, the *a*-axis lattice constant increases abruptly by a few percent for the low-temperature phase. The stress in the *a*-axis direction is hence altered from being tensile to being compressive, whereas the stress in the *c*-axis direction is maintained to be tensile. Moreover, the stress in the *a*-axis direction is reduced around T_C by alternating the domains of the low-temperature phase (α-MnAs) and high-temperature phase (β-MnAs).[4] The domain structure is visible in, for instance, Fig. 1(a) as a vertical stripe. The resultant unidirectional tensile stress is the driving force for the splitting of the films perpendicular to the *c*-axis of MnAs.

An inhomogeneous stress distribution that emerges during wet chemical etching of MnAs films generates a similar quasiperiodic array of cracks that run orthogonal to the *c*-axis.[8–10] The stress in the films changes nonuniformly during the etching because of the large difference in the etch rates between α- and β-MnAs.[8] The crack period was observed to be 5–6 times the film thickness and implies that the strain relaxation by the cracking is nearly complete. The etching-induced cracking occurs when the thickness is larger than 100 nm, i.e., much smaller than h_c. The stress imbalance apparently enhances the cracking.[10] Therefore, the change in the stress distribution at T_C in the course of the postgrowth cooling, which is sudden in comparison to the slow accumulation of the thermal stress, is similarly anticipated to trigger a fracture.[11,12]

The above-mentioned crack lines that stretch perpendicular to the *c*-axis are, in fact, zigzag lines consisting of short inclined segments, see the right-hand side crack in Fig. 1(c). The length of the segments increases several orders of magnitude with the film thickness. The films considerably thicker than h_c hence fracture along straight lines that are inclined with respect to the *c*-axis of MnAs. (We refer to these cracks as type II.) The inclination angle is about 57°, see Fig. 1(b), often with a distribution around it.

The broken pieces of the MnAs films are firmly attached to the substrates as the cracks stop at the MnAs–GaAs interface, see Fig. 1(c). As the fracture is localized in the MnAs films, the inclination angle of ≈57° is considered to be given by the mechanical properties of MnAs. The GaAs substrates merely provide the stress to crack the overgrown films and play no explicit role in establishing the direction of crack propagation. The trajectory of a crack is, in general, determined by the presence of a weak plane. While the cracks are not aligned to in-plane high symmetry directions of MnAs, they are typically vertical with respect to the surface plane, i.e., the crack surfaces are $(11\bar{2}l)$ oriented. (We cannot rule out the possibility that the vertical inclination was unrecognizable due to the small thickness.) The inclination angles for the $(11\bar{2}4)$ and $(11\bar{2}5)$ planes are, respectively, 52.5° and 58.5°, and so the surfaces exposed by the cracking do not correspond to low-index planes.

Nonetheless, the $(11\bar{2}4)$ plane, see Fig. 2(b), may play an important role for the cracking. The $(11\bar{2}4)$ plane is nonpolar. Nonpolarity is generally favored for a cracking plane as breaking ionic bonds cost energy. The high atom density of the $(11\bar{2}4)$ plane is also advantageous as less number of atomic bonds needs to be broken. When a weak plane determines the trajectory of a crack, the crack tip is, in general, subject to in-plane and out-of-plane shear deformations. The shear stress gives rise to a kinking of the crack.[13] Therefore, it may happen that cracking is initiated by the $(11\bar{2}4)$ plane and the trajectory deviates from the plane in the course of propagation. That is, the tensile stress in the *c*-axis direction could account for the increase in the angle from 52.5°. The maximum polarity expected for the *C* plane of MnAs due to the alternating Mn and As planes in the *c*-axis direction, see Fig. 2(a), may be responsible for the short zigzag pattern of

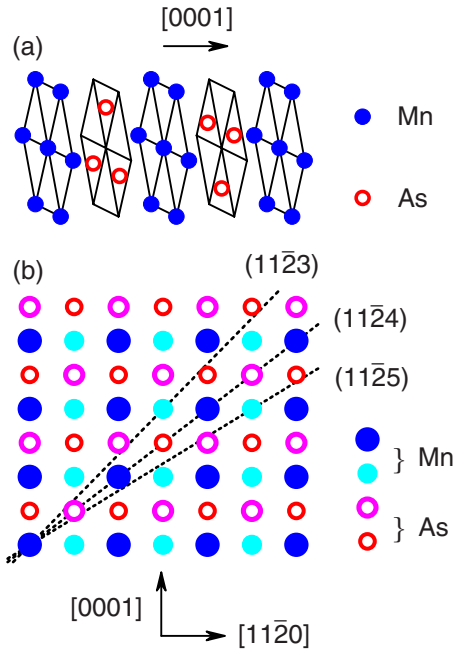

FIG. 2. (Color online) (a) Hexagonal crystal structure of MnAs. (β-MnAs is orthorhombic.) The [0001] direction is indicated. Mn and As atoms are shown by the filled and open circles, respectively. (b) Illustration of the MnAs(1$\bar{1}$00) plane. The [0001] and [11$\bar{2}$0] directions are indicated. Mn and As atoms are shown by the filled and open circles, respectively. Each has two components placed at different depths. The dotted lines indicate the (11$\bar{2}$3), (11$\bar{2}$4), and (11$\bar{2}$5) planes. The (11$\bar{2}$3) and (11$\bar{2}$4) planes are nonpolar.

the type-I cracks. Although the splitting occurs nominally orthogonal to the *c*-axis, the films strongly disfavor exposing the *C* plane.

Another possible mechanism for the tilting of the cracks is the large anisotropy of the modulus of elasticity *E* of MnAs. The orientational dependence of *E* is described for hexagonal crystals by the expression

$$E^{-1} = s_{11}\sin^4\theta + s_{33}\cos^4\theta + (s_{44} + 2s_{13})\sin^2\theta\cos^2\theta, \tag{2}$$

where θ is the angle with respect to the *c*-axis. Using the value of the elastic compliance constants s_{ij} in Ref. 14, the modulus in the *c*-axis direction $E_c = 110$ GPa is estimated to be about three times larger than that in the *a*-axis direction $E_a = 38$ GPa. In this scenario, cracking does not occur orthogonal to the *c*-axis as *G* does not exceed the fracture toughness. The angle of $\theta = 57°$ is interpreted to correspond to the condition of $G(\theta) \approx K_f$. Although we do not consider this to be the case for the crack inclination in the MnAs/GaAs(001) system as we discuss below, the anisotropy of *E* could modify the cracking characteristics.

When the type-I and type-II cracks coexist, they form alternating domains in the *c*-axis direction, as shown in Fig. 1(b). The type-I crack lines are discontinued or diverted when they approach the type-II cracks. The type-II cracks are hence suggested to be generated at early stages of the sample cooling. The type-I cracks are produced later in the regions sandwiched by the segments of the type-II cracks when the phase-transition stress sets in at T_C. This implies that the thermal expansion mismatch is solely responsible for the

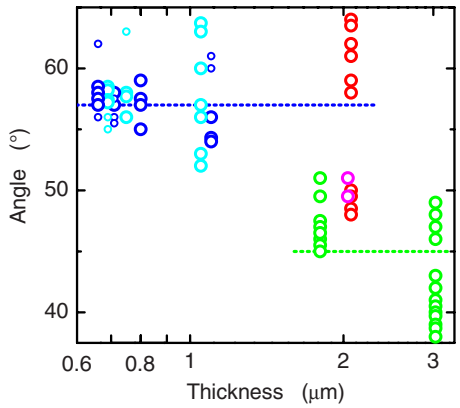

FIG. 3. (Color online) Variation in the inclination angle of the cracks with respect to the *c*-axis of MnAs when the film thickness is changed. The two horizontal lines indicate characteristic crack angles (57° and 45°) in the two fracture regimes.

type-II cracks. The tensile stress is approximately isotropic in this circumstance, and so the *c*-axis direction of MnAs has no significance (in the continuum model). (To be precise, the thermal mismatch in the *c*-axis direction is nearly twice larger than that in the *a*-axis direction.[4]) In reality, however, the hexagonal structure of MnAs provides weak plane directions that presumably lead to the crack angle of about 57°. Nevertheless, the type-II cracks still retain the form of a quasiperiodic array of parallel zigzag lines. The unidirectionality in the stress arising from the structural phase transition at T_C cannot be ignored. This may suggest the following alternative mechanism for the elongation of the individual inclined segments of the zigzag crack lines when the thickness is increased: As a film becomes tougher for a larger thickness, the fracture occurs by a cleavinglike process splitting a weak plane over a long distance rather than the breaking that is forced to be perpendicular to the *c*-axis by the direction of the stress.

In Fig. 3, we show the variation in the crack angle with the film thickness. The distribution of the crack angle widens as the film thickness increases. However, as indicated by the upper horizontal line in Fig. 3, the median inclination angle seems to be independent of the thickness, at least up to 1.1 μm. (As we show below, the cracking enters a different regime when the thickness further increases.) When an individual film cracks with a number of inclination angles, we observe that the crack angle generally does not change in each zigzag crack line. We also find that the zigzag crack lines inclined by different angles usually do not merge or cross with each other, see Fig. 1(d). The cracks having different inclination angles are thus indicated to be formed at separate stages during cooling. The angle is uniquely related to the state of the stress at the temperature of the cracking. This may account for the thickness-independent median angle of 57°, i.e., the cracking occurs most frequently when the stress reaches a certain common value, for which the crack propagation angle happens to be 57°.

B. Substrate fracture regime

When the thickness is beyond 2 μm, the strain energy becomes large enough to fracture the GaAs substrates, as

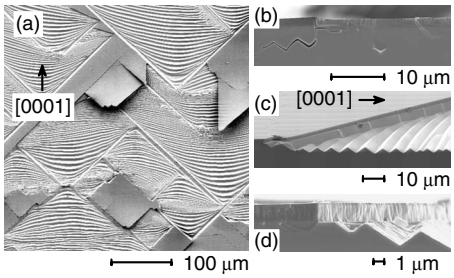

FIG. 4. Scanning electron micrographs of a MnAs film on GaAs(001). The film thickness is 1.8 μm. The *c*-axis of MnAs is aligned in the vertical direction in (a) and in the horizontal direction in (b)–(d).

shown in Fig. 4(a). We emphasize that the fracture of these very thick films progresses as cracking in the brittle substrate rather than delamination along the interface.[15,16] The MnAs–GaAs interface bonding is thus indicated to be strong. The condition for a crack that entered the substrate turning and propagating parallel to the interface, see Fig. 4(b), is $K_s/\sigma_f h^{1/2} < 0.58$, where K_s is the fracture toughness of the substrate.[2] We thus find $K_s = 0.8K_f$. A crack propagates in the substrate instead of along the interface if $K_s < 2.1K_i$.[2] The fracture toughness K_i of the interface is hence estimated to be $K_i > 1.7K_f$.

When the thickness increases to the regime of the substrate fracture, the crack pattern changes to diamond shapes. The inclined segments are much longer than the period when the cracks formed a quasiperiodic array. The diamond-shaped cracking may thus appear to be inefficient from the viewpoint of the strain relaxation, i.e., it leaves behind a large amount of residual strain. In fact, the MnAs films are no longer seriously stressed in the further course of the cooling once the substrates fracture. The transition in the crack pattern is actually a manifestation that the residual stress is lowered to the extent that the phase-transition stress cannot generate the type-I cracks when the temperature crosses T_C.

The crack angle in the very thick films changes to about 45°. In Fig. 3, the crack angle is seen to switch between two values indicated by the horizontal lines when the thickness crosses the critical value of 2 μm. As the films peel off in the form of MnAs/GaAs composites when the films are thicker than 2 μm, the crack angle in this regime is determined by the mechanical properties of the hybrid system. The in-plane crack angle should generally depend on the volume ratio between MnAs and GaAs in the composite flakes. The depth of the crack path from the MnAs–GaAs interface is typically several times the film thickness.[2] The mechanical properties of GaAs are thus expected to be dominant in settling the crack angle as, in addition to the large volume fraction, GaAs is harder than MnAs. That the fracture pattern is approximately fourfold symmetric suggests that the crack angle of ≈45° originates from the cubic symmetry of the GaAs substrate. [The ratio of the lattice constants of MnAs in the *c*- and *a*-axis directions is $c/a = 1.53$, and so fourfold symmetric patterns are rather unusual for MnAs unless the 45° cracks are related to the $(11\bar{2}3)$ plane, which has a tilt angle of 44.4°, see Fig. 2(b).] It may be noteworthy that the side surfaces of MnAs films revealed by the 45° cracks are often inclined in the vertical direction, Fig. 4(c). Because of the large film thickness, the microstructures on the surface of the cracks can be clearly seen, as shown in Fig. 4(d). The roughness is elongated in the direction normal to the substrate, suggesting that the crack propagated by repetition of cleavages and jumps.

The fracture lines delineated on the substrate surface are oriented along the [100] and [010] directions instead of following the cleavage directions [110] and $[1\bar{1}0]$ of GaAs(001). This indicates that the cracking in the substrate is initiated by the other cleavage planes (011) and (101). The inclination of these planes with respect to the plane normal is plausibly the cause of the corrugations imprinted on the cracked GaAs surfaces, see Fig. 4(a). The height variation of the corrugations is larger than the thickness of the MnAs films. In general, the depth of the trajectory along which a crack propagates is stable as any deviation from this path is suppressed by the shear stress produced by the perturbation itself.[16] As shown in Fig. 4(c), the cracks propagate in the GaAs substrate tracing a fairly regular sawtooth profile in the vertical direction. The quasi-instability is presumably a consequence of the guiding by the weak (011) and (101) planes.

The substrate fracture is initiated at two opposite edges of the diamond-shaped cracked pieces and propagates along the [110] direction of the substrate. This directionality originates from the MnAs overlayer. The diamond-shaped cracks are essentially an assemble of zigzag lines. Thus, the peeling starts from the corners of the zigzag lines. The peeled sections bend upward due to the rolling of a strained bilayer, thereby assisting the in-plane propagation of the cracks in the substrate. The progress of the peeling in the direction along the *c*-axis of MnAs gives rise to the characteristic stripe pattern on the fractured GaAs surfaces.

IV. DELAMINATION OF ANNEALED FILMS

Due to the large thermal expansion of MnAs, cracking occurs also when films undergo an annealing process. The low growth temperature for epitaxial MnAs films implies that originally crack-free films can suffer from the cracking and/or delamination from substrates at the temperature, for instance, for alloying Ohmic contacts to the GaAs substrates. Moreover, annealing process is detrimental for MnAs as the material is oxidized at even lower temperatures.[17,18] Spin injection from a MnAs film to a GaAs-(Al,Ga)As quantum well was demonstrated in Ref. 19, in which the contacts to the substrate were prepared without annealing to avoid the delamination and oxidation. As we demonstrate in this section, we have discovered a method for annealing that circumvents these problems.

Figure 5(a) shows the surface image of a 25-nm-thick MnAs film after an annealing at 400 °C. Instead of the tensile stress that causes the cracking in thick films, the film needs to relieve a nearly isotropic compressive stress. As a consequence, the film exhibits roughly circularly shaped buckling and associated delamination, as shown in Fig. 5(b).[6] Although the film is more than one order of magnitude thinner than the critical thickness for the cracking of thick films, the delamination is found to be unavoidable. This readiness for fracture is presumably related to the fact that MnAs is

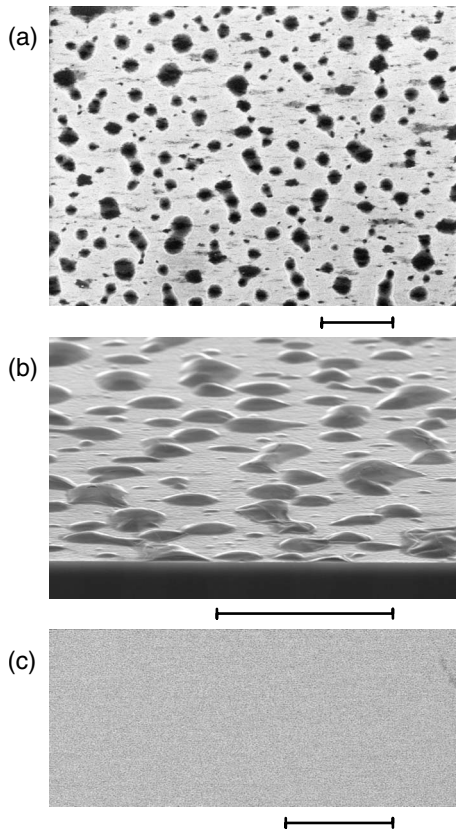

FIG. 5. Scanning electron micrographs of MnAs films on GaAs(001) after an annealing at 400 °C for 10 min. The MnAs films are 25 nm thick. The film in (c) is capped by a Mn layer, whereas the film in (a) and (b) are uncapped. The scale bars are 10 μm long.

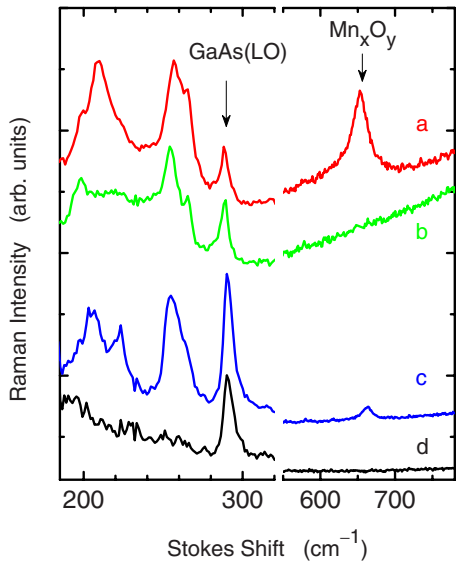

FIG. 6. (Color online) Raman spectra of MnAs films after an annealing at 400 °C. Top two curves were obtained from a 25-nm-thick MnAs film, which was almost completely oxidized by the annealing, see Figs. 5(a) and 5(b). Curve a was taken from a buckle associated with delamination. Curve b was taken from the area attached to the substrate, i.e., outside the buckles. Curves c and d were obtained from the MnAs film capped by a Mn layer shown in Fig. 5(c). Curve d was taken after the surface semitransparent layer had been removed by scratching. The arrows indicate the peaks associated with a manganese oxide (Mn_xO_y) and the LO phonon in the GaAs(001) substrates. The curves are offset for clarity.

oxidized during the annealing. The film became highly resistive after the annealing although MnAs is a metal. Almost complete oxidation of the film is hence evidenced. The low oxidation temperature is a serious problem for high-temperature processing of MnAs films.

The top two curves in Fig. 6 show the Raman spectra of the delaminated film. Curve a was obtained from the buckle. The peak at 650 cm^{-1} is attributed to a manganese oxide Mn_xO_y.[20,21] This peak was absent in the area where the film was attached to the substrate, curve b. The reason for the absence of Mn_xO_y is unclear at present. The peaks that appear below 280 cm^{-1} are also ascribed to the oxidized MnAs film. The latter peaks are detected both for the buckles and outside the buckles.

We have found that both the delamination and the oxidation of MnAs films are suppressed by a Mn capping. The image in Fig. 5(c) was taken from the surface of a Mn-capped MnAs film after an annealing. Here, no buckles are present. The delamination is thus demonstrated to be circumvented. The surface was covered by a yellow-colored semitransparent layer. The Raman spectrum shown by curve c in Fig. 6 indicates this surface layer to be an oxidized Mn layer. In the area where the top semitransparent layer was scratched away, the peaks in the Raman spectra vanished except for the one associated with the GaAs substrate, curve d. The disappearance of the Raman signal indicates that the underlying layer remained to be metallic. The metallic conduction in the MnAs film was confirmed by resistance measurements as we show below. The Mn layer is thus seen to act as a protection layer to prevent the oxygen penetration. The absence of the delamination in Fig. 5(c) is attributed to the adhesion by the buried nonoxidized MnAs film. When the annealing temperature was reduced to 200 °C, even the oxidation of the Mn-capping layer was negligibly small although the annealing was carried out for 40 min (not shown). Without the Mn capping, MnAs films suffer from oxidation even at 200 °C.[17]

While the Mn layer protects the underlying MnAs film from oxidation during annealing, we have observed a phenomenon in which the top oxide layer is suggested to cause an oxidation of the underlying MnAs film at room temperature. In Fig. 7, we show the time dependence of the resistance of the Mn-capped MnAs film. The annealing process was completed at time $t=0$. Although the sample was kept at room temperature in H_2 atmosphere, the resistance increased gradually. As shown by the thin solid curve, the time evolution obeys the power law with an exponent of 4.1. In Ref. 22, manganese oxides were reported to act as a catalyst to enhance the oxidation of arsenic, forming an As_2O_3 microcrystal know as arsenolite. We, therefore, speculate that manganese oxides (such as MnO, Mn_2O_3, Mn_3O_4, and MnO_2) add extra oxygen to the underlying MnAs film by means of changing their own composition.

Interestingly, the oxidation does not take place if the resistance is not measured. For instance, we turned off the current for 3 h during the measurement run, as marked in Fig. 7. Although the resistance increase still progressed during the period, the change was only two-thirds in comparison to the expected power-law evolution. The resistance increase rate when the current had been turned on again was also

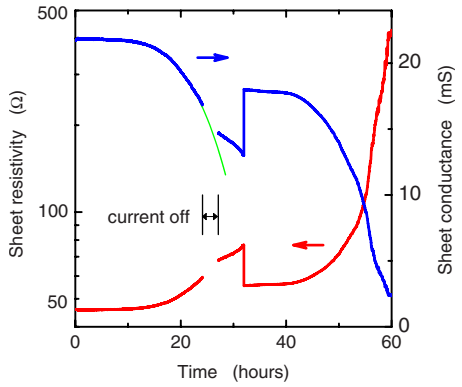

FIG. 7. (Color online) Time dependence of the sheet resistivity and the sheet conductivity of a Mn-capped MnAs film. An annealing process at 400 °C for 10 min was completed at time zero. The sample was afterwards kept in H_2 atmosphere at room temperature. The current density for the measurement was about 4×10^{-4} A/m. The current was turned off for 3 h during the indicated interval. The thin curve shows a fit to the power-law dependence with an exponent of 4.1.

reduced. The oxidation thus appears to be activated when a current flows through the MnAs film. (The current density for the measurement was about 4×10^{-4} A/m.) Such an activation of oxidation by supplying electrons has been reported for other systems.[23] Displacing an arsenic atom in the MnAs crystal by an oxygen atom involves a release of the arsenic atom. Activating this process requires an electron as oxygen is a group-VI element and arsenic is a group-V element.

During the measurement run presented in Fig. 7, we encountered an abrupt resistance drop. The gradual increase in the resistance with time after this abrupt change proceeded as if the resistance measurement began at $t=32$ h. The fact that the resistance can drop discontinuously almost to the initial value suggests that the resistance increase is caused by an oxidation not of the entire MnAs film but in a highly localized area which lies somewhere along the current path. The resistance may drop if the current-blocking section is "punctured" for some reason (for instance, an electrical surge).

V. SUMMARY

We have investigated the fracture of epitaxial MnAs films grown on GaAs(001) substrates during cooling to room temperature. The unusually large thermal expansion of MnAs gives rise to a cracking when the films are thicker than 0.5 μm. The films peel off from the substrates when the thickness exceeds 2 μm by extending the cracks into the substrates. Characteristic in-plane inclination angles of the cracks are found to exist in each of the fracture regimes. These angles manifest the important role in the crack initiation and propagation of specific weak planes of the single-crystal films and substrates. We have also shown that annealing process even at moderate temperatures results in a delamination of the MnAs films from the substrates. The delamination occurs even when the films are remarkably thin because of the oxidation of MnAs. We have demonstrated that Mn-capping prevents the oxidation of the MnAs films, thereby enabling us to avoid the delamination. Finally, we have presented a phenomenon in which the oxidized Mn-cap layer oxidizes the underlying MnAs film through an electrically activated process.

ACKNOWLEDGMENTS

Most of the MnAs films used in this study were grown under the supervision of L. Däweritz and K. H. Ploog. The authors thank O. Brandt for helpful conversations.

[1] M. D. Thouless, Annu. Rev. Mater. Sci. **25**, 69 (1995).
[2] M. D. Thouless, J. Vac. Sci. Technol. A **9**, 2510 (1991).
[3] K. Bärner, Phys. Status Solidi B **88**, 13 (1978).
[4] L. Däweritz, Rep. Prog. Phys. **69**, 2581 (2006).
[5] L. Däweritz, F. Schippan, A. Trampert, M. Kästner, G. Behme, Z. M. Wang, M. Moreno, P. Schützendübe, and K. H. Ploog, J. Cryst. Growth **227–228**, 834 (2001).
[6] A. S. Argon, V. Gupta, H. S. Landis, and J. A. Cornie, Mater. Sci. Eng., A **107**, 41 (1989).
[7] M. S. Hu, M. D. Thouless, and A. G. Evans, Acta Metall. **36**, 1301 (1988).
[8] Y. Takagaki, E. Wiebicke, T. Hesjedal, H. Kostial, C. Herrmann, L. Däweritz, and K. H. Ploog, Appl. Phys. Lett. **83**, 2895 (2003).
[9] Y. Takagaki, E. Wiebicke, J. Mohanty, T. Hesjedal, L. Däweritz, and K. H. Ploog, Physica E (Amsterdam) **24**, 115 (2004).
[10] Y. Takagaki, E. Wiebicke, L. Däweritz, and K. H. Ploog, J. Solid State Chem. **179**, 2271 (2006).
[11] G. Fischer and W. B. Pearson, Can. J. Phys. **36**, 1010 (1958).
[12] S. Haneda, N. Kazama, Y. Yamaguchi, and H. Watanabe, J. Phys. Soc. Jpn. **42**, 1201 (1977).
[13] M. D. Thouless, H. C. Cao, and P. A. Mataga, J. Mater. Sci. **24**, 1406 (1989).
[14] M. Dörfler and K. Bärner, Phys. Status Solidi A **17**, 141 (1973).
[15] M. D. Drory, M. D. Thouless, and A. G. Evans, Acta Metall. **36**, 2019 (1988).
[16] Z. Suo and J. W. Hutchinson, Int. J. Solids Struct. **25**, 1337 (1989).
[17] Y. Takagaki, L. Däweritz, and K. H. Ploog, Phys. Rev. B **75**, 035213 (2007).
[18] M. Ramsteiner, H. J. Zhu, and L. Däweritz, Appl. Phys. Lett. **79**, 2411 (2001).
[19] M. Ramsteiner, H. Y. Hao, A. Kawaharazuka, H. J. Zhu, M. Kästner, R. Hey, L. Däweritz, H. T. Grahn, and K. H. Ploog, Phys. Rev. B **66**, 081304 (2002).
[20] F. Buciuman, F. Patcas, R. Craciun, and D. R. T. Zahn, Phys. Chem. Chem. Phys. **1**, 185 (1999).
[21] C. M. Julien, M. Massot, and C. Poinsignon, Spectrochim. Acta, Part A **60**, 689 (2004).
[22] Y. Takagaki, E. Wiebicke, M. Ramsteiner, L. Däweritz, and K. H. Ploog, Appl. Phys. A: Mater. Sci. Process. **76**, 837 (2003).
[23] I. Jimeńez, M. Moreno, J. A. Martín-Gago, M. C. Asensio, and J. L. Sacedón, J. Vac. Sci. Technol. A **12**, 1170 (1994).